

ADVANCING SEISMIC CAPACITY CURVE PREDICTIONS WITH A META-MODELING FRAMEWORK FOR STRUCTURAL SYSTEMS

MAHAN SAMIADEL¹, FARAHNAZ SOLEIMANI²

¹Oregon State University
1501 SW Campus Way, Corvallis, Oregon, USA
samiadem@oregonstate.edu

² Oregon State University
1501 SW Campus Way, Corvallis, Oregon, USA
farahnaz.soleimani@oregonstate.edu

Key words: Seismic Performance Prediction, Incremental Dynamic Analysis, Stacked Machine Learning, Seismic Capacity Curves, Cascadia Subduction Zone, Probabilistic Performance-based Assessment

Abstract. Predicting accurate seismic capacity curves for reinforced concrete (RC) bridges is essential for assessing seismic performance and resilience, particularly in earthquake-prone regions such as the Pacific Northwest. The Cascadia Subduction Zone megathrust earthquake presents a critical threat to such infrastructure, yet traditional approaches often fail to capture the nonlinearities and high-dimensional relationships between structural parameters and seismic responses. While single-model machine learning (ML) techniques have shown promise, their limited robustness and generalizability hinder their effectiveness. To address these challenges, this research introduces a stacked machine learning framework to enhance the prediction of capacity curves, specifically using column drift ratios as a key measure of structural performance under seismic loading. The proposed framework systematically evaluates various regression models to construct an optimized meta-model by selecting the best-performing algorithms based on predictive accuracy and generalizability. Incremental Dynamic Analysis (IDA) is performed on randomized RC bridge samples, with input parameters systematically varied using the Latin Hypercube Sampling technique to generate a diverse training dataset. Ground motion suites tailored to Cascadia-specific long-duration seismic characteristics ensure the framework's regional applicability. Advanced ensemble and boosting-based regression algorithms, such as Random Forest and Extreme Gradient Boosting, are tested and the top-performing models are combined into the meta-model. This stacked approach addresses the limitations of single-model techniques by improving robustness, accuracy, and the ability to generalize across diverse structural configurations. The ML models predict capacity curves based on column drift ratios, providing precise and actionable insights into structural performance. To ensure interpretability, Explainable AI (XAI) techniques, such as SHapley Additive exPlanations (SHAP), are used to rank the importance of input parameters, offering actionable insights for seismic design and retrofit strategies. This stacked machine learning approach offers several advantages, including the ability to model complex, nonlinear relationships and produce accurate capacity curve predictions for RC bridges. Results

demonstrate that the framework enhances the reliability of seismic risk assessments and reduces computational demands, empowering engineers and decision-makers to design, evaluate, and retrofit infrastructure with greater confidence. By overcoming the limitations of existing methodologies, this research highlights the transformative potential of stacked machine learning in advancing seismic risk assessment practices and strengthening infrastructure resilience.

1 INTRODUCTION

Reinforced concrete (RC) bridges are critical components of transportation infrastructure, and their reliable seismic performance is essential for public safety and post-earthquake recovery. In regions such as the Pacific Northwest, where the Cascadia Subduction Zone poses a major seismic threat, accurately predicting the nonlinear response of these structures has become increasingly important. Reliable predictions are vital to support informed design, evaluation, and retrofitting strategies aimed at enhancing bridge resilience.

A fundamental pillar of seismic performance assessment is the development of capacity curves that relate engineering demand parameters, such as column drift ratios (CDR) [1], to increasing levels of seismic intensity. These curves form the basis for performance-based seismic design and risk evaluation. However, generating accurate capacity curves is computationally intensive and often requires incremental dynamic analysis (IDA), a method widely recognized for its effectiveness in assessing bridge performance across a broad range of seismic demands [2,3]. Despite its robustness, the complexity and computational demands of IDA have historically limited its widespread adoption in routine engineering practice, although advances in computational power have alleviated some of these constraints [3].

Traditional methods for predicting the seismic capacity of RC bridges, such as empirical formulas and simplified analytical models, often struggle to capture the highly nonlinear, dynamic behavior observed during strong earthquakes. These approaches may inadequately account for critical failure mechanisms, such as progressive yielding and redistribution of internal forces, potentially leading to unreliable seismic assessments [2,4]. While physics-based finite element models provide more detailed analyses, they remain computationally expensive and face challenges in generalizing across diverse structural configurations and loading conditions [5].

In recent years, machine learning (ML) techniques have emerged as promising tools for seismic performance prediction [6-8]. However, standalone ML approaches, such as artificial neural networks (ANNs) [9,10], tend to lack robustness and generalizability. For instance, an ANN-based model developed to predict the seismic fragility of RC bridges achieved improved accuracy but was constrained by the quality and representativeness of its training data, limiting its broad applicability [11]. These challenges highlight the need for more advanced modeling strategies capable of addressing the complexities inherent in seismic performance prediction of RC bridges.

To overcome the limitations of traditional, individual ML models, this study proposes a stacked ML framework that combines algorithms such as Extreme Gradient Boosting and Random Forests to predict seismic performance of RC bridges. Using IDA results from randomized bridge configurations subjected to ground motions representative of Cascadia Subduction Zone events, a robust training dataset is developed. The framework also

incorporates SHapley Additive exPlanations (SHAP) analysis to ensure model transparency and identify key factors influencing structural drift under seismic loading.

2 METHODOLOGY

This study integrates physics-based simulation and ML to develop a predictive framework for estimating seismic capacity curves of RC bridges. The methodology involves: (1) modeling RC bridges using finite element analysis; (2) performing IDA with Cascadia-specific ground motions; (3) training ML models using simulation results; and (4) employing a stacked meta-model (SMM) with SHAP analysis for interpretability. The overall workflow is illustrated in Figure 1.

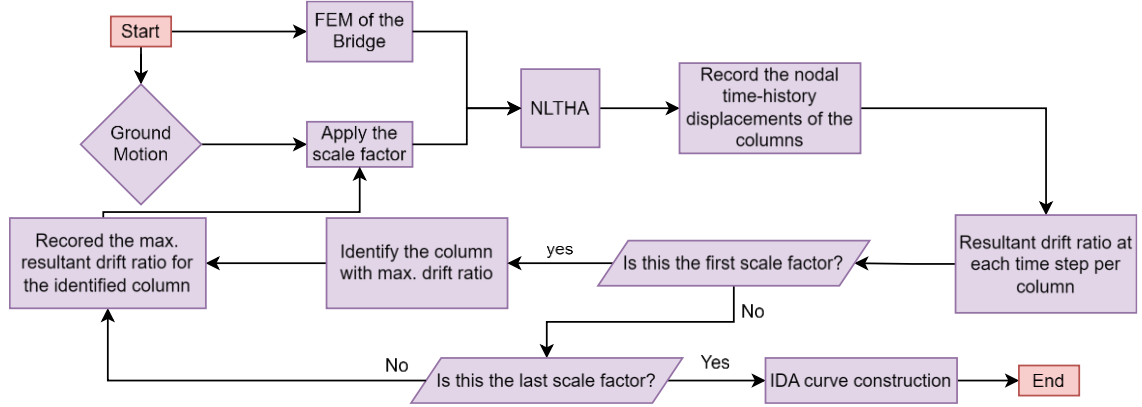


Figure 1: Workflow of the study to create IDA curves

2.1 Bridge Modeling and Input Parameter Sampling

Thirty multi-span continuous (MSC) RC bridge samples were selected from Ramanathan's thesis [12], representing typical post-1990 bridge designs with integral tee-girder superstructures, diaphragm abutments, and single-column bents. Each bridge includes a monolithically cast deck and girders, forming a continuous system without expansion joints or restrainer cables at intermediate supports. This design enhances stiffness and seismic resilience by reducing vulnerabilities such as pounding or unseating. The superstructure consists of five girders with moderate deck thicknesses and typical girder dimensions informed by statistical trends observed in the broader bridge population. The center span is approximately 1.4 times the length of the end span.

The supporting columns are 60-inch diameter circular RC sections reinforced with uniformly spaced #8 longitudinal bars confined by transverse steel ties or spirals. Foundations are modeled as pile-supported caps to simulate realistic soil-structure interaction, while diaphragm abutments are designed to engage passive backfill soil during seismic events, providing additional restraint against deck displacements. To capture the variability in structural characteristics, geometric and material properties were systematically varied using Latin Hypercube Sampling (LHS) [13,14]. The resulting input parameter space, summarized in Tables 1 and 2, includes properties such as concrete strength, reinforcement details, soil stiffness, deck mass multipliers, and ground motion intensity measures. Finite element models

were developed in OpenSees using fiber-based beam-column elements with material and geometric nonlinearities to simulate the full range of seismic behavior.

Each bridge was modeled using a high-fidelity three-dimensional finite element discretization in OpenSees. Fiber-based beam-column elements with both material and geometric nonlinearities were employed to accurately simulate expected seismic demands on both superstructure and substructure components. This modeling framework enabled the generation of detailed simulation data across a wide range of structural configurations and seismic intensities, forming the foundation for the subsequent machine learning analysis.

2.2 Incremental Dynamic Analysis (IDA)

IDA [15] was employed to evaluate the seismic demand of RC bridge samples under varying levels of earthquake intensity. Ten suites of ground motion records representative of the Cascadia Subduction Zone were applied in both longitudinal and transverse directions. Unlike traditional time-history analysis that uses unscaled records, IDA involves systematically scaling each ground motion across a range of intensity levels (here, peak ground acceleration (PGA)) to capture the full response spectrum from elastic behavior to dynamic instability or collapse.

Each ground motion was scaled using the following scale factor:

$$SF_i = \frac{i \cdot g}{PGA_j} \quad (0.1 \leq i \leq 2.5) \quad (1)$$

where SF_i is the scale factor for the i^{th} increment, g is gravitational acceleration, and PGA_j is the peak ground acceleration of the j^{th} ground motion. This formulation yields a series of scaled ground motions ranging from 0.1g to 2.5g in increments of 0.1g, applied to each bridge model. The scaled motions were applied to finite element models (FEM) in OpenSees, and dynamic analyses were conducted.

The maximum CDR was selected as the primary engineering demand parameter (EDP) for characterizing structural response. At each time step, the resultant drift ratio was computed from the relative displacements at the top and bottom nodes of each column in both longitudinal (Δ_L) and transverse (Δ_T) directions:

$$CDR_R = \frac{\sqrt{\Delta_L^2 + \Delta_T^2}}{H} \quad (2)$$

where H is the column height, and the relative displacements are calculated using the followings.

$$\Delta_L = D_{top_L} - D_{bottom_L} \quad (3)$$

$$\Delta_T = D_{top_T} - D_{bottom_T} \quad (4)$$

Here, D_{top_L} , D_{bottom_L} , D_{top_T} , and D_{bottom_T} are the recorded displacements of the top and bottom nodes in the longitudinal and transverse directions, respectively.

For each bridge-ground motion combination, 25 scaled simulations were performed, generating continuous IDA curves that capture the relationship between seismic intensity and structural demand. These curves served as the target dataset for subsequent machine learning model development.

2.3 Machine Learning Techniques

2.3.1 Input Features

Eighteen input features encompassing material properties (such as concrete strength), geometrical characteristics of the bridge samples (including span lengths, column heights, and section dimensions), and seismic characteristics were used to predict the maximum resultant CDR (see Table 1). Their statistical distribution is provided in Table 2. This comprehensive input space enables the ML models to learn the complex interactions that govern seismic response. Four ML base models were trained to predict maximum CDR values.

Table 1: Input variables along with notations and units.

| Variable | Notation | Unit |
|---|-----------|------------|
| Concrete strength | fc | ksi |
| Steel strength | fys | ksi |
| Ultimate passive soil pressure | F_ult | ksi |
| Average (initial) passive soil stiffness | K_a | kips/in/ft |
| Abutment pile effective stiffness | K_eff | kips/in/ft |
| Multiplication factor for deck mass | ms | percentage |
| Damping ratio | dr | - |
| The time step of the applied ground motion | dt_gm | sec |
| The duration of the applied ground motion | D_gm | sec |
| The PGA of the applied ground motion | or_PGA | g |
| Bent cap stiffness | unt_wt | kip/in |
| Foundation rotational stiffness | soil_prop | kip-in/rad |
| Maximum span length | max_span | ft |
| Width of the bridge | width | ft |
| Super-structure girder spacing | spacing | ft |
| Number of #8 column longitudinal reinforcing bars | rebar_num | - |
| Spacing of #4 stirrups in the column | tran_spac | in |
| Scaled PGA | sc_PGA | g |

Table 2: Statistical description of the input variables

| Variable | Minimum | Maximum | Mean | Std. Dev. | Skewness |
|----------|---------|---------|-------|-----------|----------|
| fc | 3.33 | 6.10 | 4.73 | 0.70 | 0.06 |
| fys | 57.22 | 83.34 | 67.61 | 6.03 | 0.62 |
| F_ult | 0.01 | 0.08 | 0.04 | 0.02 | 0.19 |
| K_a | 26.34 | 49.53 | 37.70 | 6.91 | 0.02 |
| K_eff | 37.51 | 98.45 | 68.64 | 18.01 | 0.10 |

| | | | | | |
|-----------|----------|----------|----------|---------|-------|
| ms | 1.11 | 1.30 | 1.21 | 0.06 | -0.07 |
| dr | 0.01 | 0.07 | 0.04 | 0.01 | 0.06 |
| dt_gm | 0.01 | 0.03 | 0.01 | 0.01 | 0.71 |
| D_gm | 52.06 | 423.49 | 246.83 | 108.68 | 0.13 |
| Or_PGA | 0.001393 | 0.22 | 0.07 | 0.07 | 1.09 |
| unt_wt | 15.96 | 58.43 | 32.12 | 10.51 | 0.84 |
| soil_prop | 3019810 | 28364659 | 11618353 | 7187887 | 0.74 |
| max_span | 40.03 | 130.00 | 73.74 | 29.48 | 0.94 |
| width | 30.00 | 43.64 | 35.76 | 5.00 | 0.35 |
| spacing | 6.00 | 8.73 | 7.15 | 1.00 | 0.35 |
| rebar_num | 20.00 | 162.00 | 85.73 | 48.04 | 0.01 |
| tran_spac | 3.00 | 3.45 | 3.04 | 0.12 | 3.07 |
| sc_PGA | 40.03 | 130.00 | 73.74 | 29.48 | 0.94 |

2.3.2 Base Predictive Models

To predict the maximum resultant drift ratios based on both structural characteristics and seismic input parameters, four ML base models were employed. Specifically, Random Forest (RF) (an ensemble learning [16] method based on bagging) and three boosting-based algorithms, Gradient Boosting (GB), Extreme Gradient Boosting (XGBoost), and Light Gradient Boosting Machine (LightGBM) [17], were developed and trained. Each model's predictive performance was evaluated individually using standard regression metrics, including the coefficient of determination (R^2 score), Root Mean Squared Error (RMSE), and Mean Absolute Error (MAE).

RF [18] is an ensemble learning method that improves prediction accuracy and reduces overfitting by averaging the outputs of multiple decision trees. Each tree is trained on a bootstrapped subset of the data and, at each node split, considers a randomly selected subset of input features. The trees are grown to full depth without pruning to maximize variance among individual learners. The final prediction for a given input x is obtained by averaging the predictions of all trees:

$$\hat{y} = \frac{1}{K} \sum_{k=1}^K h(x, \Theta_k) \quad (5)$$

where $h(x, \Theta_k)$ is the prediction from the k^{th} tree, constructed using a random vector Θ_k , and K is the total number of trees in the forest.

GB [19] is a powerful ensemble technique that builds a strong predictive model by sequentially adding weak learners, typically decision trees, such that each new model focuses on correcting the mistakes made by the previous ones. Gradient Boosting proceeds by initializing the prediction with a constant (e.g., the mean of the target variables), then adding corrections step-by-step. At iteration t , a new model $h_t(x)$ is trained to approximate the negative gradient of the loss function with respect to the current prediction $\hat{f}_{t-1}(x)$ which is equivalent to the residual $y - \hat{f}_{t-1}(x)$ for squared error loss. The model is updated as:

$$\hat{f}_t(x) = \hat{f}_{t-1}(x) + \lambda \cdot h_t(x) \quad (6)$$

where $\lambda \in (0, 1]$ is the learning rate (also called shrinkage), which controls the contribution of each new model, and $h_t(x)$ is typically a shallow regression tree fitted to the residuals. This iterative refinement allows Gradient Boosting to capture complex nonlinear patterns while maintaining flexibility and control over overfitting.

XGBoost [20] is an optimized and scalable implementation of GB that builds a model by sequentially decision trees, each aiming to correct the errors made by the previous ones. XGBoost distinguishes itself through several key features: its ability to handle sparse input data efficiently, a regularized objective function that mitigates overfitting, and the use of second-order (Hessian) gradient information to accelerate and stabilize the learning process. At each boosting iteration t , a new regression tree $\hat{f}_t(x)$ is added to refine the prediction from the previous iteration $\hat{y}_i^{(t-1)}$. The updated prediction is given by:

$$\hat{y}_i^t = \hat{y}_i^{(t-1)} + f_t(x_i) \quad (7)$$

This approach enables XGBoost to achieve high predictive accuracy while maintaining computational efficiency, making it specifically suitable for large-scale and high-dimensional datasets.

LightGBM is a GB framework that constructs an ensemble of decision trees by sequentially adding one tree at a time to correct the prediction errors of the existing model. Similar to traditional gradient boosting, each new tree is trained on the negative gradients (i.e., residuals) of a specified loss function, such as mean squared error, computed from the previous iteration's predictions. The final prediction for an input x_i is the cumulative output of all trees:

$$\hat{y}_i = \sum_{j=1}^T f_j(x_i) \quad (8)$$

where \hat{y}_i is the predicted value for input x_i and each f_j represents a regression tree learned at iteration j . What distinguishes LightGBM is its emphasis on computational speed and memory efficiency, making it particularly well-suited for large-scale and high-dimensional datasets. It achieves this through techniques such as histogram-based splitting and leaf-wise tree growth with depth constraints, enabling faster training and improved scalability without compromising accuracy.

2.3.3 Stacked Meta-Model (SMM)

To enhance robustness and generalizability, the base models were integrated into a stacked ensemble. Stacking combines the predictions of individual learners using a secondary model (meta-model) that learns how to best weight each base prediction. In this study, Ridge Regression was used as the meta-model due to its ability to manage multicollinearity and prevent overfitting by penalizing large coefficients. This stacked approach leverages the strengths of each base learner to deliver more accurate and reliable drift predictions across the full range of bridge and seismic input parameters.

Stacking [21] is a method that improves predictive accuracy by combining multiple base models through a secondary learner called meta-model. Instead of selecting a single best model, stacking uses the predictions from several base models trained on original input features as inputs to a meta-model, which learns how to optimally combine them. For regression tasks, this

is typically done by minimizing mean squared error. Unlike simple averaging, stacking accounts for the specific biases and errors of each base model, allowing the meta-model to adaptively weight their contributions. In this study, Ridge Regression is used as the meta-model because of its ability to prevent overfitting through L2 regularization and handle multicollinearity among base model outputs.

2.4 Model Interpretability with SHAP

To interpret the contributions of each input feature to the predicted CDR, SHAP [12], a game theory-based method, was employed. SHAP assigns each feature a value representing its marginal contribution to a given prediction. It provides both local (instance-specific) and global (model-wide) explanations while maintaining consistency (i.e., a feature's SHAP value will not decrease if its influence increases). In this study, SHAP was used to rank feature importance, understand how specific parameters, such as column height and concrete strength, affect predictions, and enhance transparency and trustworthiness of the ML outputs for engineering applications.

SHAP [22], a widely used method in Explainable AI (XAI), is grounded in cooperative game theory and provides a mathematically rigorous framework for interpreting ML models. It treats each input feature as a "player" and the model prediction as the "payout", aiming to fairly distribute the prediction among features based on their marginal contributions. SHAP values represent these contributions across all possible feature combinations, ensuring a consistent and equitable measure of feature importance. A key strength of SHAP is its consistency: if a feature's contribution to a prediction increases, its SHAP value will not decrease. This property, along with its ability to provide both global and local interpretability, makes SHAP a powerful tool for understanding and validating model behavior.

4 RESULTS AND DISCUSSION

Figure 2 shows the IDA curves generated for the 30 bridge samples subjected to Cascadia Subduction Zone ground motions. Each curve represents the variation of maximum column resultant drift ratio with increasing PGA for a specific ground motion record. As expected, the drift response generally increases with PGA, transitioning from elastic behavior at lower intensities to nonlinear and near-collapse behavior at higher intensities. The divergence among the curves highlights the variability in structural response due to both differences in bridge configurations and seismic input characteristics.

At lower PGA values (below $\sim 0.02g$ – $0.04g$), most bridge samples maintain small drift ratios, indicating elastic or lightly nonlinear behavior. Beyond this range, drift ratios escalate more rapidly, signaling the onset of significant nonlinear deformations. In some cases, curves show abrupt increase in drift, suggesting local instability or strength degradation mechanisms under high seismic demand. The variability across the IDA curves underscores the importance adopting a probabilistic modeling framework that accounts for both structural and seismic uncertainties, rather than relying on deterministic analyses, for more reliable vulnerability assessment.

The ML models developed in this study demonstrated strong performance in predicting the maximum CDR, used as the EDP. Predictive models developed using RF, GB, XGBoost, LightGBM, and SMM were evaluated for their ability to predict maximum CDR. The SMM,

which integrates predictions from the base models using Ridge Regression, demonstrated enhanced generalizability while maintaining the high accuracy of the individual learners. Its use of Ridge as the meta-learner allowed for effective aggregation without introducing additional model complexity, making it well-suited for deployment across diverse structural and seismic scenarios.

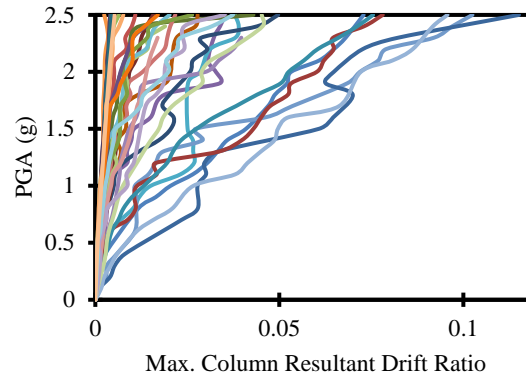


Figure 2: IDA curves related to 30 bridge samples

To evaluate model performance, a 10-fold cross-validation procedure was used. In this method, the dataset was randomly divided into 10 equal subsets; in each iteration, nine were used for training and one for testing, with the process repeated across all subsets. This technique reduces variance due to random data partitioning and provides a more reliable and unbiased assessment of model performance. Alongside the mean values of R^2 , RMSE, and MAE, the standard deviations of these metrics were also computed to assess stability and robustness of the models.

Table 3 presents the evaluation metrics for all five models. R^2 score ranges from 0.975 to 0.985, indicating strong predictive capability across all approaches. The lowest RMSE and MAE were achieved by XGBoost (0.235% and 0.13%, respectively), followed closely by GB and RF. Although LightGBM showed slightly reduced performance, its results remained within acceptable bounds. The SMM model achieved an R^2 of 0.980, with low variability across metrics, reflecting its ability to blend the strengths of the base models and produce consistent predictions. While its individual accuracy was marginally below XGBoost, the stacked model's enhanced generalizability makes it more suitable for deployment across diverse bridge configurations and seismic scenarios that is a critical advantage in practical applications.

Table 3: Evaluation metrics for various ML models

| Model | R^2 | RMSE | MAE |
|----------|-------|---------|---------|
| RF | 0.977 | 0.00273 | 0.00133 |
| GB | 0.979 | 0.00228 | 0.00122 |
| XGBoost | 0.985 | 0.00235 | 0.0013 |
| LightGBM | 0.975 | 0.00292 | 0.00154 |
| SMM | 0.98 | 0.00263 | 0.00187 |

Figure 3 further illustrates the performance of the SMM model. Subplot (a) compares the predicted versus actual drift ratios and shows strong agreement with the 45-degree reference line with most predictions falling within $\pm 10\%$ of the actual values, and nearly all within $\pm 20\%$. This indicates the model's high accuracy across a wide range of seismic intensities. Complementing this, subplot (b) presents the residuals distribution, which is narrow, symmetric, and centered around zero. The residuals exhibit a narrow spread and resemble a normal distribution, suggesting that the model maintains consistent performance without systematic bias across different levels of drift ratio. These plots reinforce the reliability and stability of the SMM approach in capturing structural responses.

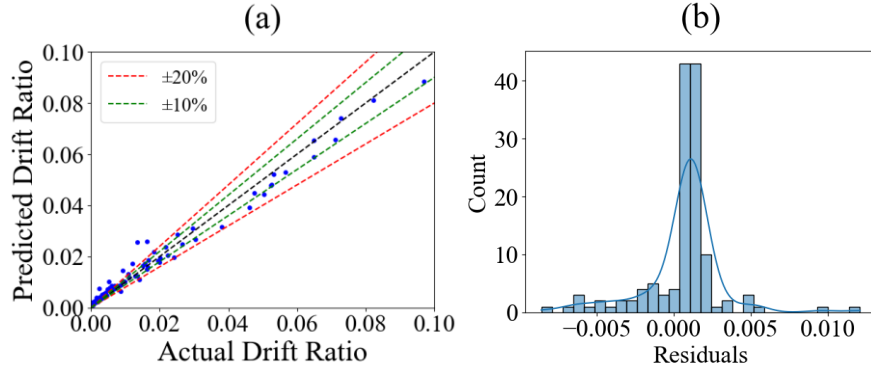


Figure 3: SMM Results: (a) Predicted vs. actual values (b) Residuals Distribution

Figure 4 displays the SHAP summary plot for the SMM model, providing insight into the influence of each input feature on the predicted drift ratio. Each point represents the SHAP value of a specific feature for an individual instance, with color indicating the feature's magnitude: red for high values and blue for low values.

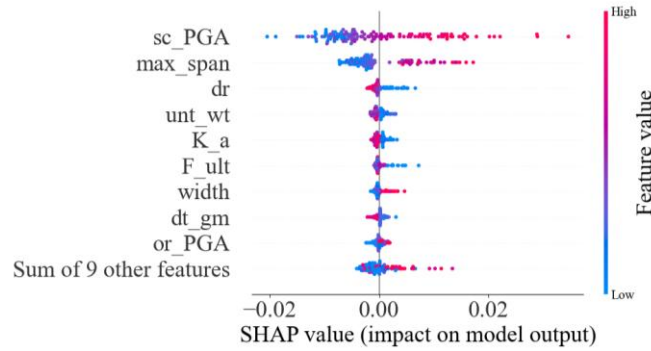


Figure 4: SHAP values of input variables for SMM

Scaled PGA (sc_PGA), maximum span length (max_span), and damping ratio (dr) emerged as the most influential features, as indicated by their broad SHAP value distributions. A positive SHAP value indicates that the feature increases the predicted outcome, whereas a negative value suggests it contributes to a lower prediction. For instance, higher values of sc_PGA typically increase the predicted drift, while geometric parameters such as girder spacing and column reinforcement contribute with varying directional impacts depending on their range. This confirms the model's ability to capture nonlinear feature interactions. Features with moderate influence, such as column width and bent cap stiffness (unt_wt), also contribute meaningfully to prediction outcomes. Overall, this SHAP analysis provides valuable interpretability,

confirming that seismic intensity and structural geometry are the dominant drivers in the model's decision-making process.

5 CONCLUSION

This study proposed a data-driven framework for predicting the maximum CDR of RC bridges subjected to seismic loading, with a particular focus on ground motions representative of the Cascadia Subduction Zone. IDA was conducted on a suite of bridge models with systematically varied geometric and material properties. This dataset, along with 25 intensity levels for each bridge-ground motion pair, was used to train and evaluate several ML models, including Random Forest, Gradient Boosting, XGBoost, LightGBM, and a Stacked Meta-Model.

Among the individual models, XGBoost achieved the highest prediction accuracy, while the SMM offered improved superior generalizability across diverse structural configurations and seismic inputs. SHAP analysis further enhances interpretability, identifying scaled PGA, span length, and damping ratio as dominant drivers of drift response. These findings demonstrate that ensemble-based ML methods can effectively capture complex nonlinear relationships in structural behavior, offering a computationally efficient and interpretable alternative to traditional simulation-heavy approaches. Overall, the proposed framework enables rapid, accurate, and transparent estimation of seismic demand parameters. It shows strong potential for integration into performance-based design workflows and seismic risk assessment processes, particularly for regions exposed to high-consequence seismic hazards like the Cascadia Subduction Zone.

REFERENCES

- [1] S. Zehsaz, S. Kameshwar, and F. Soleimani, "Kernel-based Column Drift Ratios Prediction in Highway Bridges," presented at the The 10th World Congress on New Technologies, Aug. 2024. doi: 10.11159/icceia24.164.
- [2] A. H. M. M. Billah and M. S. Alam, "Seismic performance evaluation of multi-column bridge bents retrofitted with different alternatives using incremental dynamic analysis," *Engineering Structures*, vol. 62–63, pp. 105–117, Mar. 2014, doi: 10.1016/j.engstruct.2014.01.005.
- [3] A. Mahmoudi Moazam, N. Hasani, and M. Yazdani, "Incremental dynamic analysis of small to medium spans plain concrete arch bridges," *Engineering Failure Analysis*, vol. 91, pp. 12–27, Sep. 2018, doi: 10.1016/j.engfailanal.2018.04.027.
- [4] J. B. Mander, R. P. Dhakal, N. Mashiko, and K. M. Solberg, "Incremental dynamic analysis applied to seismic financial risk assessment of bridges," *Engineering Structures*, vol. 29, no. 10, pp. 2662–2672, Oct. 2007, doi: 10.1016/j.engstruct.2006.12.015.
- [5] P. Chomchuen and V. Boonyapinyo, "Incremental dynamic analysis with multi-modes for seismic performance evaluation of RC bridges," *Engineering Structures*, vol. 132, pp. 29–43, Feb. 2017, doi: 10.1016/j.engstruct.2016.11.026.
- [6] F. Soleimani and D. Hajializadeh, "State-of-the-Art Review on Probabilistic Seismic Demand Models of Bridges: Machine-Learning Application," *Infrastructures*, vol. 7, no. 5, p. 64, Apr. 2022, doi: 10.3390/infrastructures7050064.

- [7] F. Soleimani, B. Vidakovic, R. DesRoches, and J. Padgett, "Identification of the significant uncertain parameters in the seismic response of irregular bridges," *Engineering Structures*, vol. 141, pp. 356–372, Jun. 2017, doi: 10.1016/j.engstruct.2017.03.017.
- [8] F. Soleimani, "Analytical seismic performance and sensitivity evaluation of bridges based on random decision forest framework," *Structures*, vol. 32, pp. 329–341, Aug. 2021, doi: 10.1016/j.istruc.2021.02.049.
- [9] F. Soleimani and X. Liu, "Artificial neural network application in predicting probabilistic seismic demands of bridge components," *Earthq Engng Struct Dyn*, vol. 51, no. 3, pp. 612–629, Mar. 2022, doi: 10.1002/eqe.3582.
- [10] J. Atkins, F. Soleimani, and D. Hajializadeh, "Quantifying Seismic Resilience of Highway Bridges: A Case Study using Bayesian Neural Network," presented at the The 10th World Congress on New Technologies, Aug. 2024. doi: 10.11159/icceia24.136.
- [11] C. Huang and S. Huang, "Predicting capacity model and seismic fragility estimation for RC bridge based on artificial neural network," *Structures*, vol. 27, pp. 1930–1939, Oct. 2020, doi: 10.1016/j.istruc.2020.07.063.
- [12] K. N. Ramanathan, *Next generation seismic fragility curves for California bridges incorporating the evolution in seismic design philosophy*. [Online]. Available: <http://hdl.handle.net/1853/44883>
- [13] F. Soleimani, "Propagation and quantification of uncertainty in the vulnerability estimation of tall concrete bridges," *Engineering Structures*, vol. 202, p. 109812, Jan. 2020, doi: 10.1016/j.engstruct.2019.109812.
- [14] F. Soleimani, *Fragility of California Bridges – Development of Modification Factors*. 2017. [Online]. Available: <http://hdl.handle.net/1853/58300>
- [15] D. Vamvatsikos and C. A. Cornell, "Incremental dynamic analysis," *Earthq Engng Struct Dyn*, vol. 31, no. 3, pp. 491–514, Mar. 2002, doi: 10.1002/eqe.141.
- [16] F. Soleimani and D. Hajializadeh, "Bridge seismic hazard resilience assessment with ensemble machine learning," *Structures*, vol. 38, pp. 719–732, Apr. 2022, doi: 10.1016/j.istruc.2022.02.013.
- [17] M. Samiadel and F. Soleimani, "Data-Driven Strength Prediction of Recycled Aggregate Concrete: Insights from Boosting-Based Machine Learning Models," presented at the The 10th World Congress on Civil, Structural, and Environmental Engineering, Apr. 2025. doi: 10.11159/icsect25.170.
- [18] L. Breiman, "Random Forests," *Machine Learning*, vol. 45, no. 1, pp. 5–32, 2001, doi: 10.1023/A:1010933404324.
- [19] A. Natekin and A. Knoll, "Gradient boosting machines, a tutorial," *Front. Neurorobot.*, vol. 7, 2013, doi: 10.3389/fnbot.2013.00021.
- [20] T. Chen and C. Guestrin, "XGBoost: A Scalable Tree Boosting System," in *Proceedings of the 22nd ACM SIGKDD International Conference on Knowledge Discovery and Data Mining*, San Francisco California USA: ACM, Aug. 2016, pp. 785–794. doi: 10.1145/2939672.2939785.
- [21] D. H. Wolpert, "Stacked generalization," *Neural Networks*, vol. 5, no. 2, pp. 241–259, Jan. 1992, doi: 10.1016/S0893-6080(05)80023-1.
- [22] S. Lundberg and S.-I. Lee, "A Unified Approach to Interpreting Model Predictions," 2017, *arXiv*. doi: 10.48550/ARXIV.1705.07874.